

Concentration of Radiation Displacement Defects in $\text{Ca}_{0.28}\text{Ba}_{0.72}\text{Nb}_2\text{O}_6$ Crystal as Function of Electrons or Neutrons Energy

P. POTERA*

Institute of Materials Science and Engineering of Rzeszow University, Pigonia 1, 35-310 Rzeszów, Poland

Received: 03.01.2022 & Accepted: 01.04.2022

Doi: [10.12693/APhysPolA.141.585](https://doi.org/10.12693/APhysPolA.141.585)

*e-mail: ppotera@ur.edu.pl

This work is devoted to the calculation of the concentration of the radiation displacement defects in $\text{Ca}_{0.28}\text{Ba}_{0.72}\text{Nb}_2\text{O}_6$. The main purpose of this work is to determine the dependence of the concentration of defects induced by electrons and neutrons on $\text{Ca}_{0.28}\text{Ba}_{0.72}\text{Nb}_2\text{O}_6$ on their energy. The dependencies were determined on the basis of calculations made using the Monte Carlo method realized in the Atom Collision Cascade Simulation program. These dependencies can be approximated to known analytical functions. Energy dependence of radiation displacement defects concentrations as well as cascade function versus the energy of electrons and neutrons are discussed.

topics: CBN, radiation displacement defects, irradiation, crystal defects

1. Introduction

As one of the members of lead-free materials, tungsten bronze family materials (such as $\text{Sr}_{1-x}\text{Ba}_x\text{Nb}_2\text{O}_6$) have been widely researched because of their superior electro-optic, dielectric, piezoelectric, ferroelectric, and pyroelectric properties [1–6]. The $\text{Ca}_x\text{Ba}_{1-x}\text{Nb}_2\text{O}_6$ compound (CBN), which was first mentioned as a ceramic material in 1959 [7], is the Ca analog of $\text{Sr}_{1-x}\text{Ba}_x\text{Nb}_2\text{O}_6$ (SBN) compounds. The main advantage of the CBN compound is the high Curie temperature (above 220°C [8, 9]), higher than that of SBN. It was shown in [10] that the solid solution of $\text{Ca}_{0.28}\text{Ba}_{0.72}\text{Nb}_2\text{O}_6$ shows the best stability because the CBN phase formation was easiest at $x = 0.28$.

In recent years, CBN compounds have received continuously increasing interest, in which most works are mainly focused not only on ceramics [11, 12] but also on thin films and single crystals [13–17]. For example, yttrium-doped CBN crystal is a good candidate as an ultra short laser medium [14], and neodymium-doped CBN crystal is an excellent candidate for a self-frequency converter solid-state laser [18] or a diode pumped laser [19]. Solid-state lasers for space-based Lidar systems for monitoring atmospheric parameters are a part of the payload of satellites following polar orbit of several hundred km during 3–10 years [20]. Depending upon the orbit, exposure levels of ionizing radiation can reach upward of 10 kGy.

The interaction of primary cosmic rays with the Earth's atmosphere leads to the formation of secondary radiation, the main component of which are:

γ quanta, high-energy protons, neutrons, and electrons. The measured energy of the secondary elementary particles of cosmic rays in the atmosphere practically does not exceed 1000 MeV with flux depending on their energy (at airplane altitude, the significant part of electrons has energy in the range of 10–400 MeV [21], and neutrons in the range of 0.1–200 MeV [22], wherein the flux of neutrons prevails the flux of electrons). It was shown [23] that γ irradiation (dose of 3 kGy) leads to a significant change in the absorption of CBN crystal. It is known that such changes in the absorption induced by ionizing radiation, resulting in the formation of radiation defects, lead to a reduction in the laser efficiency [24]. On the other hand, color centers (which can be produced among others by irradiation) are widely used in quantum information, quantum sensing, micro- and nano-optics and other relevant fields [25–27].

From this point of view, displacement damage caused by electrons or neutrons in microelectronic and optoelectronic devices can have a significant impact on the performance of these devices. Therefore, it is important to predict not only the displacement damage profile, but also precisely its magnitude. Unfortunately, the influence of electrons and neutrons on the CBN has not been practically studied.

Within the framework of the binary collision approximation (BCA), the concentration of displaced atoms can be solved (i) analytically, as in the Kinchin–Pease or NRT damage production models [28, 29], and (ii) numerically, as in the DART

code [30] or via Monte Carlo simulations (e.g. as it is the case for the SRIM code [31]). The models mentioned use threshold displacement energy. The Kinchin–Pease and NRT models are applied to centers composed of one type of ion. In turn, using the program SRIM to compute the production rate of the displacement per atom (DPA) induced by neutrons within the BCA framework is time-consuming, similar in the DART code. Additionally, the SRIM software cannot be used for modelling the electrons stopping.

Marlowe [32], on the other hand, does not use displacement energy. Instead, it uses only the lattice binding energy and then pairs the interstitial atoms with vacancies. Based on the configuration of the Frenkel pairs, Marlowe classifies these pairs as close, near, or distant, where distant pairs are considered as permanent replacements. Unfortunately, this separation is an ad hoc assumption, and the results do not agree with molecular dynamics calculations. Furthermore, most models do not take into account the fact that at high energy of the primary knocked-out atom (PKA) a significant part of the kinetic energy of the PKA is transferred to the electron subsystem, leading mainly to the ionisation of the medium [33].

The present work is devoted to the calculation of the concentration of radiation displacement defects (RDD) in CBN crystals as a function of electrons and neutrons energy according to the atom–atom collision cascades model [34]. The Monte Carlo method is used (based on the assumptions of the Kinchin–Pease binary collision model [28]), taking into account the energy losses of the ions knocked out for ionization of the environment.

2. Methods

During irradiation by the neutrons or electrons, the energy of the particle is transferred to the atom of material, which is knocked out. If the energy of the particle is high, the primary knocked-out atom can displace subsequent atoms. There are three most important physical parameters describing radiation damage: the threshold displacement energy T_d , the differential cross section $\frac{d\sigma_d(E,T)}{dT}$ for transfer of the recoil energy T to crystal atom from a particle with energy E , and cascade function $\nu(T)$ defined as the number of displaced atoms per one PKA with recoil energy T .

The situation is more complicated in the case of materials composed of different types of atoms. The concentration of displaced atoms in the atom sublattice of the j -type (per unit fluence of the particle), created due to the initial displacement of one atom of the i -type (primary knocked-out atom — PKA) with energy T_i , was determined as [35]

$$n_{dij/F} = n_i \int_{T_{di}}^{T_{\max,i}} dT_i \frac{d\sigma_{di}(E,T)}{dT} \nu_{ij}(T_{di}). \quad (1)$$

Here n_i is the concentration of i -type atoms in the lattice, $\frac{d\sigma_{ai}(E,T)}{dT}$ is the differential cross-section of the elastic scattering of the irradiation particle on the atom of i -type that results in the transfer of recoil energy T (in the case of electron irradiation, the McKinley–Feschbach approximation formula [36] was used, and for neutron irradiation, the hard spheres model was used [34]), $T_{\max,i}$ is the maximum possible recoil energy of i -type atoms, T_{di} is the threshold displacement energy of i -type atoms, and $\nu_{ij}(T_i)$ is a cascade function, which describes the number of displaced j -type atoms per one PKA of the i -type with energy T_i . The total concentration of displacements in the j -sub-lattice ($n_{dj/F}$) is a sum of partial concentrations $n_{dij/F}$.

The calculations were performed in the Atom Collision Cascade Simulation program (ACCS) [37]. The detailed procedure of calculation and determination of the cascade functions was described in [38]. The ACCS program gives results much faster than most other programs. It takes into account the fact that for an energy of the knocked ion greater than A [keV] (where A is the mass number of the knocked ion), most of its kinetic energy goes into the ionization of the environment [39]. It should be mentioned that the work [35] shows that the RDD concentration calculated with the ACCS programme agrees well with the experimentally determined concentration of RDD for gadolinium gallium garnet.

The unit that is frequently used for measuring radiation damage is the displacement per atom (DPA). It is a measure of the amount of radiation damage in irradiated materials. The DPA (per unit particle fluence) of j -type ions can be derived as

$$\text{DPA}(j) = \frac{n_{d,j/F} M}{N_A \rho}, \quad (2)$$

where ρ — density [g/cm³], N_A — Avogadro number, and M — molar mass [g/mol].

The computations of concentrations of RDP in CBN crystal were performed for irradiation by neutrons and electrons with particle energy ranging 0.01–200 MeV (for neutrons) and 1–500 MeV (for electrons). The threshold displacement energy T_d values for ions taken from [40–42] are given in Table I. The density of the CBN was 5.321 g/cm³ [43]. The mass number and atomic number were taken from the periodic table. The ionic radii were taken from the database of ionic radii [44].

3. Results and discussions

In Figs. 1 and 2 the dependence of the calculated exemplary cascade function $\nu_{Ca,j}$ as a function of the energy of electrons and neutrons is presented. This cascade function has a tendency to saturation with the energy of the particle. The same remark applies to other cascade functions, e.g., $\nu_{Ba,j}$, $\nu_{Nb,j}$, and $\nu_{O,j}$.

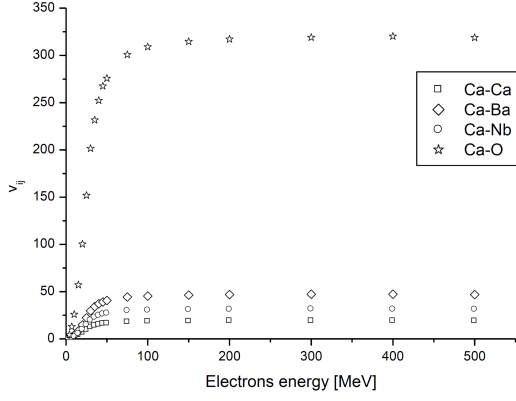
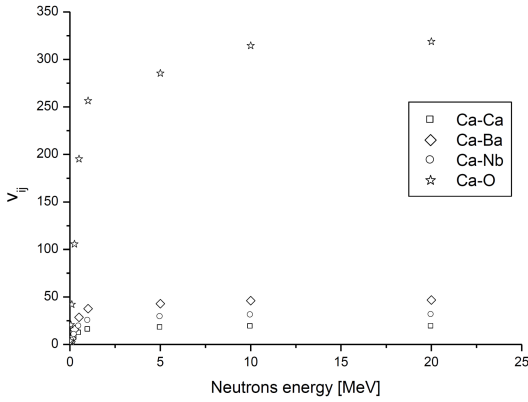

 Fig. 1. Cascade functions for Ca PKA ion (ν_{Ca_j}) in the case of electron irradiation.

 Fig. 2. Cascade functions for Ca PKA ion (ν_{Ca_j}) in the case of neutron irradiation.

TABLE I

The threshold displacement energy for Ca, Ba, Nb, and O ions.

Ion	T_d [eV]	Ref.
Ca	25	[40]
Ba	21	[41]
Nb	75 (average value)	[42]
O	45 (average value)	[40]

The cascade functions can be approximated to the function

$$\nu_{ij}(E) = \nu_{ij,1} + \frac{\nu_{ij,0} - \nu_{ij,1}}{1 + \left(\frac{E}{E_{ij}}\right)^p}, \quad (3)$$

 where $\nu_{ij,0}$, $\nu_{ij,1}$, p and E_{ij} are constants, and E is the particle energy.

 It is important to note that the production of defects in the oxygen sublattice is much more effective than in the cation sub-lattice. The values of approximation parameters of cascade functions ($\nu_{ij,0}$, $\nu_{ij,1}$, E_{ij} , and p) calculated for electrons and neutrons in the Microcal Origin program are given in Tables II and III, respectively.

TABLE II

The parameters of approximation of cascade functions for electron irradiation.

Cascade function	$\nu_{ij,0}$	$\nu_{ij,1}$	E_{ij} [MeV]	p
ν_{CaCa}	1.2261	17.60868	25.62076	2.94303
ν_{CaBa}	0.57146	46.23233	25.67524	2.94155
ν_{CaNb}	0.33911	30.74726	25.68154	2.962
ν_{CaO}	3.68229	313.5978	25.63152	2.96458
ν_{BaCa}	0.49274	55.76946	85.73112	2.84337
ν_{BaBa}	2.45246	147.0254	86.40346	2.80402
ν_{BaNb}	0.96429	98.24138	86.4429	2.79796
ν_{BaO}	6.94888	998.2405	86.64794	2.81984
ν_{NbCa}	0.43847	38.49858	58.99875	2.9575
ν_{NbBa}	1.28083	101.1573	59.15417	2.9254
ν_{NbNb}	1.55324	67.24715	58.91853	2.93267
ν_{NbO}	7.17295	684.3246	59.0067	2.96893
ν_{OCa}	0.08264	7.90587	10.54362	2.85527
ν_{OBa}	0.13459	20.60128	10.54259	2.84099
ν_{ONb}	0.03626	13.76286	10.60833	2.82461
ν_{OO}	2.43665	140.5417	10.49783	2.85539

TABLE III

The parameters of approximation of cascade functions for neutron irradiation.

Cascade function	$\nu_{ij,0}$	$\nu_{ij,1}$	E_{ij} [MeV]	p
ν_{CaCa}	1.25276	17.49577	0.3829	1.49748
ν_{CaBa}	0.58475	45.77707	0.38309	1.47335
ν_{CaNb}	0.36765	30.61474	0.38953	1.48834
ν_{CaO}	3.33674	310.9886	0.38078	1.47481
ν_{BaCa}	-0.83513	58.80674	2.52131	1.14697
ν_{BaBa}	-0.27998	154.0401	2.73044	1.17189
ν_{BaNb}	-0.98298	102.7789	2.68776	1.1606
ν_{BaO}	-14.01143	1049.27	2.71421	1.14689
ν_{NbCa}	0.08085	42.03805	3.19859	1.05917
ν_{NbBa}	0.44656	110.1879	3.27389	1.04714
ν_{NbNb}	1.21485	73.25276	3.31206	1.05372
ν_{NbO}	1.31757	749.347	3.26569	1.06057
ν_{OCa}	0.1669	7.78563	0.07476	1.53279
ν_{OBa}	0.4254	20.21805	0.07509	1.5906
ν_{ONb}	-0.67046	14.38144	0.06824	1.4781
ν_{OO}	-7.94753	150.377	0.06598	1.48487

 For electron irradiation, the values of $\nu_{ij,0}$, $\nu_{ij,1}$, E_{ij} strongly depend on type of sub-lattice, but values of parameter p are practically the same for each sub-lattice (2.79–2.86). The same remark applies to neutron irradiation, but the dispersion of the value of parameter p is greater ($p = 1.05$ – 1.50).

TABLE IV

The displacement defect concentration per unit fluence of irradiation particles (in 10^{-22} DPA) and saturation energy $E_{j,\text{max}}$ [MeV] for each sublattices of CBN crystal.

j (sublattice)	Parameters	Electrons	Neutrons
Ca	$\text{DPA}(j)$	0.42444	6.70039
	$E_{j,\text{sat}}$	11.20267	3.94439
Ba	$\text{DPA}(j)$	1.70938	17.63117
	$E_{j,\text{sat}}$	5.3556	4.23546
Nb	$\text{DPA}(j)$	1.0253	11.74912
	$E_{j,\text{sat}}$	8.1642	3.97888
O	$\text{DPA}(j)$	5.4131	119.18624
	$E_{j,\text{sat}}$	23.04675	3.99952

It should be noted that although T energy for oxygen ions is about 2 times higher than T_d for Ca and Ba ions, due to the much higher concentration of oxygen ions in the crystal, the formation of RDP in the oxygen sub-network is more effective. For example, in the oxide sub-lattice of the CBN crystal, the PKA cations produce a few to a dozen times more displacement than in the cation sub-lattice (7–18 times for electrons and 7–20 times for neutrons) (Table II and III).

Computed dependencies of concentrations of the displaced atoms on one particle of primary radiation in CBN crystal as a function of electron and neutron beam energy are presented in Figs. 3 and 4, respectively. The concentrations of displaced atoms in each sub-lattice ($\text{DPA}(j)$) calculated per unit fluence increased initially with the particles (electrons or neutrons) energy, and then they saturated for energy of a few to a dozen MeV.

Turns out to be that the dependence of displaced ion concentration per unit fluence in the function of particle energy can be approximated by the function

$$\text{DPA}(j) = \text{DPA}(j)_{\text{max}} \left(1 - \exp\left(-\frac{E}{E_{j,\text{sat}}}\right) \right). \quad (4)$$

The values of $\text{DPA}(j)$ and $E_{j,\text{sat}}$ calculated using the Microcal Origin program are given in Table IV. The saturation energy $E_{j,\text{sat}}$ means that the $\text{DPA}(j)$ reached 63.21% of the maximum value. The values of $E_{j,\text{sat}}$ for neutron are near 4 MeV independently on crystal sub-lattice, but for electrons are higher and depend on sub-lattice (Table IV).

The total concentrations of displaced cations for saturation area have a lower value then the number of displaced oxygen ions (for neutron irradiation, the oxygen ions are about 63% of all ions, for electron — 78% of all ions). This saturation is related to the fact that at energies of several keV and above, the knocked-out ion loses energy mainly for the ionisation of the environment.

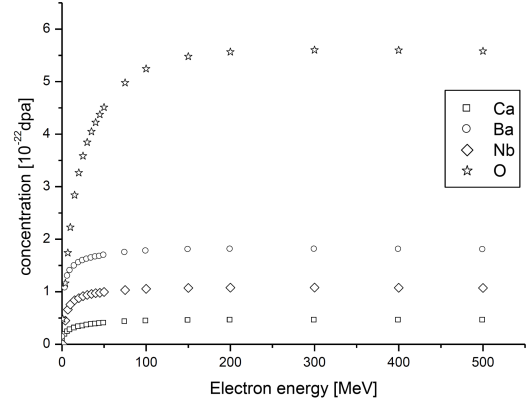


Fig. 3. Dependence of displaced ions concentrations reduced to one impinging particle in CBN crystals on electron beam energy.

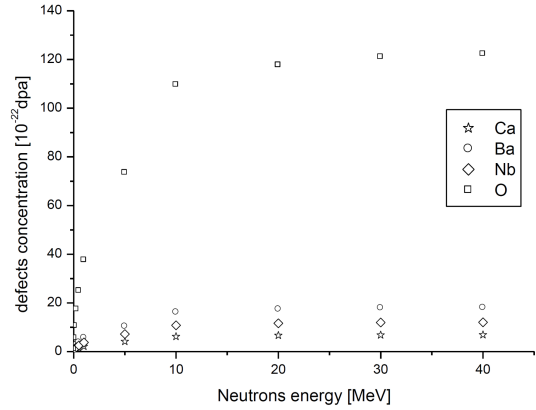


Fig. 4. Dependence of displaced ions concentrations reduced to one impinging particle in CBN crystals on neutron beam energy.

In the case of irradiation by the neutrons or electrons with particle energy corresponding to the saturation area, the concentration of RDD is about 11–22 times greater for neutrons than for electrons for each sub-lattice and 18 times greater for the total DPA concentration. For comparison, the last parameter is higher than that calculated for garnet and perovskite-like crystals (4–10 times), lower than for PbMnO_4 and sillenite crystals (25–30 times), and close to the value for YVO_4 crystal (16 times) [35, 38, 45].

The calculated values of total RDD concentration in the saturation region for electron irradiated CBN are a few times smaller than for other crystals, e.g. wulfenite, garnets, and sillenites crystals [35, 38, 45]. The same remark applies for neutron irradiated CBN crystal.

4. Conclusions

The analysis of cascade functions depending on the energy particles indicates that these functions increase with the tendency to saturation.

The calculations of concentration of RDD induced by neutron or electron irradiation in CBN crystal show that RDD are formed most effectively in the oxygen sublattice. The concentration of RDD in saturation area (which corresponds well with energy of secondary electrons and neutrons) is about 10 times larger for neutrons than for electrons, which indicates that protection against the neutron flux of potential Lidar based on CBN is very important.

Also, the calculated values of the total RDD concentration for electrons or neutrons irradiated of the CBN crystal are smaller than for wulfenite, garnets, sillenites crystals for the same energy of particles. It indicates a better resistance of the crystal to this type of radiation.

The presented calculation has shown that for a large range of energy of electrons and neutrons (above 100 MeV for electrons and above 10 MeV for neutrons), the concentration of RDD in CBN does not depend on particle energy, which may be a prospect for the use of CBN in dosimetry of high-energy neutrons or electrons.

Acknowledgments

I would like to thank Professor Sergii Ubizskii (Lviv Polytechnic) for making the ACCS program available.

References

- [1] R. Neurgaonkar, J.R. Oliver, W.K. Copy, L.E. Cross, D. Viehland, *Ferroelectrics* **160**, 265 (1994).
- [2] K. Kakimoto, T. Yoshifuji, H. Ohsato, *J. Eur. Ceram. Soc.* **27**, 4111 (2007).
- [3] Y.L. Wang, X.L. Chen, C.X. Su, Y.M. Huang, H.F. Zhou, L.L. Fang, L. Liu, *J. Mater. Sci. Mater. Electron.* **24**, 2873 (2013).
- [4] X. Hao, Y.F. Yang, *J. Mater. Sci.* **42**, 3276 (2007).
- [5] L. Tian, D.A. Scrymgeour, A. Sharan, V. Gopalan, *Appl. Phys. Lett.* **83**, 4375 (2003).
- [6] L.L. Wei, Z.P. Yang, X.K. Han, Z.H. Li, *J. Mater. Res.* **27**, 979 (2012).
- [7] I.G. Ismailzade, *Kristallografiya* **5**, 268 (1960).
- [8] Y.J. Qi, C.J. Lu., B. Chen, H.L. Song, H.J. Zhang, X.G. Xu, *Appl. Phys. Lett.* **87**, 082904 (2005).
- [9] W.L. Gao, H.J. Zhang, S.Q. Xia, B.B. Huang, D. Liu, J.Y. Wang, M.H. Jiang, L.M. Zheng, J.F. Wang, C.J. Lu, *Mater. Res. Bull.* **45**, 1209 (2010).
- [10] X. Han, L. Wei, Z. Yang, T. Zhang, *Ceram. Int.* **39**, 4853 (2013).
- [11] L. Wei, Z. Yang, X. Chao, H. Jiao, *Ceram. Int.* **40**, 5447 (2014).
- [12] L. Wei, X. Han, X. Chao, H. Jiao, Z. Yang, *J. Mater. Sci. Mater. Electron.* **25**, 1605 (2014).
- [13] J. Ruiz-Fuertes, O. Gomis, A. Segura, M. Bettinelli, M. Burianek, M. Mühlberg, *Appl. Phys. Lett.* **112**, 042901 (2018).
- [14] J. Di, X. Xu Ch. Xia, D. Zhou, Q. Sai, J. Xu, *Optik* **125**(22), 6620 (2014).
- [15] X. He, L. Gu, *Microsc. Microanal.* **23**, 1670 (2017).
- [16] S. Liu, K. Switkowski, C. Xu, J. Tian, B. Wang, P. Lu, W. Krolikowski, Y. Scheng, *Nat. Commun.* **10**, 3208 (2019).
- [17] S. Vigne, N. Hossain, S.M. Humayun Kabir, J. Margot, K. Wu, M. Chaker, *Opt. Mater. Express* **5**, 2404 (2015).
- [18] P. Molina, E. Rodríguez, D. Jaque, L.E. Bausá, J. García-Solé, H. Zhang, W. Gao Jiyang, M. Jiang, *J. Lumin.* **129**, 1658 (2009).
- [19] J. Lan, X. Huang, X. Guan, B. Xu, H. Xu, Z. Cai, X. Xu, D. Li, J. Xu, *Appl. Opt.* **56**, 4191 (2017).
- [20] T.S. Rose, M.S. Hopkins, R.A. Fields, *IEEE. J. Quant. Electron.* **31**, 1593 (1995).
- [21] M.H. Israel, *J. Geophys. Res.* **74**, 4701 (1969).
- [22] M. Kowatari, K. Nagaoka, S. Satoh, Y. Ohta, J. Abukawa, S. Tachimori, T. Nakamura, *J. Nucl. Sci. Technol.* **42**, 495 (2005).
- [23] P. Potera, Ya. Zhydachevskii, T. Lukasiewicz, *Acta Phys. Pol. A* **127**, 753 (2015).
- [24] G. Phillipps, J. Vater, *Appl. Opt.* **32**, 3210 (1993).
- [25] H. Zhang, M. Lan, G. Tang, F. Chen, Z. Shu, F. Chend, M. Li, *J. Mater. Chem. C* **7**, 12211 (2019).
- [26] Z. Ju, J. Lin, S. Shen, B. Wu, E. Wu, *Adv. Phys.* **6**, 1858721 (2021).
- [27] G. Thiering, A. Galia, *Semicond. Semimetals* **103**, 1 (2020).
- [28] G.H. Kinchin, R.S. Pease, *Rep. Prog. Phys.* **18**, 1 (1955).
- [29] K. Nordlund, S.J. Zinkle, A.E. Sand, F. Granberg, R.S. Averback, R.E. Stoller, T. Suzudo, L. Malerba, F. Banhart, W.J. Weber, F. Willaime, S.L. Dudarev, D. Simeone, *J. Nucl. Mater.* **512**, 450 (2018).
- [30] D. Simeone, O. Hablot, V. Micalet, P. Bellon, Y. Serruys, *J. Nucl. Mater.* **246**, 206 (1997).

- [31] A. Mohammadia, S.H. Mohsen, A. Asadabad, *Nucl. Instrum. Methods Phys. Res. B* **412**, 19 (2017).
- [32] M.T. Robinson, *J. Nucl. Mater.* **216**, 1 (1994).
- [33] G. Schiwetz, E. Luderer, G. Xiao, P.L. Grande, *Nucl. Instr. Methods Phys. Res. B* **175-177**, 1 (2011).
- [34] E. Friedland, *Crit. Rev. Solid State Mater. Sci.* **25**, 87 (2001).
- [35] P. Potera, *Comput. Methods Sci. Technol.* **13**, 47 (2007).
- [36] W.A. McKinley, H. Feshbach, *Phys. Rev.* **74**, 1759 (1948).
- [37] S.B. Ubizskii, *Electronics. The bulletin of State University "Lvivska Polytechnica"* **357**, 88 (1998).
- [38] P. Potera, *Centr. Eur. J. Phys.* **6**, 52 (2008).
- [39] B. Cobett, J.C. Burgoin, *Point Defect in Solid*, Vol. 2, *Semiconductors and Molecular Crystals*, Eds. J.H. Crawford, Jr, L.M. Slifkins, Plenum Press, New York 1975.
- [40] L. Veiller, J.P. Crocombette, D. Ghaleb, *J. Nucl. Mater.* **306**, 61 (2002).
- [41] V. Aubin-Chevaldonnet, D. Gourier, D. Caurant, S. Esnouf, T. Charpentier, J.M. Costantini, *J. Phys.: Condens. Matter* **18**, 4007 (2006).
- [42] A.Yu. Konobeyev, U. Fischer, Yu.A. Korovin, S.P. Simakov, *Nucl. Energy Technol.* **3**, 169 (2017).
- [43] W.L. Gao, H.J. Zhang, D. Liu, M. Xu, J.Y. Wang, Y.G. Yu, M.H. Jiang, S.Q. Sun, H. Xia, R.I. Boughton, *J. Appl. Phys.* **105**, 023507 (2009).
- [44] [Database of Ionic Radii](#).
- [45] P. Potera, *Radiat. Eff. Defects Solids* **170**, 711 (2015).